A convenient antibiotic indicator in the ozone treatment of wastewaters. An experimental and theoretical study†

Antonio J. Mota,*[a] Gonzalo Prados-Joya,[a] David Arráez-Román,[b] Manuel Sánchez-Polo,[a] Rafael Robles,[c] Mª Ángeles Ferro-García[a] and José Rivera-Utrilla*[a]

Received (in Montpellier, France) 4th March 2010, Accepted 4th May 2010
DOI: 10.1039/c0nj00171f

N-Acetyl-oxazolidin-2-one has been found to be a convenient indicator in the removal of nitroimidazole-type antibiotic contaminants in wastewaters by ozone since it is the unique product generated in the treatment of waters containing metronidazole, and it is stable against further ozonation in the experimental conditions used. The oxidative conditions imposed by the reaction do not allow isolation of any by-products, nor other stable subproducts. High-performance liquid chromatography coupled with electrospray ionization-time-of-flight mass spectrometry (HPLC-ESI-TOF(MS)) revealed the presence of simple derivatives of both metronidazole and *N*-acetyl-oxazolidin-2-one, thus indicating that both products are unambiguously connected and that, possibly, a unique reaction pathway would take place in this case. A feasible mechanism for this transformation has then been postulated, which is supported by several experimental findings such as TOC analysis and nitrate titration, both correlating well with the proposed transformation. Furthermore, this mechanism has been evaluated by DFT/B3LYP calculations, showing that the observed product is readily obtained thanks to the high exothermicity displayed by the metronidazole ozonation process.

Introduction

The use of technologies based on ozonation process for the removal of contaminants from waters is an important topic in current environmental chemistry since new contaminants are being generated, and their respective maximum permissible concentrations in the environment are not yet legally regulated. Moreover, their potential short-, medium- and long-term effects on human health are almost completely unknown.[1–3] Some of these emerging contaminants have been present in waters for decades but are only now beginning to be detected and recognized as potentially dangerous contaminants. Recent discoveries include compounds present in cosmetics, domestic products and, especially, novel pharmaceutical products designed to have enhanced effects and properties—such as those combating new diseases—and their metabolites. This is mainly due to the large variety of these compounds and their high consumption over the past few years. It has been estimated that approximately 6 million of Pharmaceuticals and Personal Care Products (PPCPs) are commercially available worldwide, with an annual 3–4% increase in the weight of pharmaceutical compounds consumed.[4]

This situation has led to the detection of high concentrations of these compounds in urban wastewaters, estimated to have an antibiotic content of 50 μg L^{-1}.[5] Their persistence in waters means that resistance to antibiotics not only affects the individuals misusing these products but also the general population.[6] The majority of these antibiotics, *e.g.*, quinolones, nitroimidazoles, and sulfonamides, have a low biodegradability[1,7] and high toxicity,[7] and show mutagenic along with carcinogenic properties.[8] Among the antibiotics, nitroimidazoles can appear in waters at concentrations of 0.1–90.2 μg L^{-1}.[9] These compounds are widely used to treat infections caused by anaerobic and protozoan bacteria, *e.g.*, *Trichomonas vaginalis* and *Giardia lamblia*.[10,11] Besides their use as antibiotics in human beings, nitroimidazoles are also added to poultry and fish feed, leading to their accumulation in the animals, in the water of fish-farms, and, especially, in effluents from meat industries.[5]

There are few data on the capacity of different treatment systems to remove nitroimidazoles, which were only recently detected in waters.[8,12] Unfortunately, as demonstrated by previous studies, conventional treatment systems[7,13]—mainly based on the use of microorganisms—have been proved to be inadequate to effectively destroy these types of organic compounds, mostly due to their complex molecular structure. It is therefore necessary to seek new technologically viable and economically feasible alternatives to effectively remove these contaminants from waters.

The main objective of this study is the analysis of the metronidazole (**1**) degradation by ozone, through the

[a] *Departamento de Química Inorgánica, Facultad de Ciencias, Universidad de Granada, Avenida de Fuentenueva, 18002-Granada, Spain. E-mail: mota@ugr.es, jrivera@ugr.es; Tel: (+34) 958 24 04 42 (AJM), (+34) 958 24 85 23 (JRU)*
[b] *Departamento de Química Analítica, Facultad de Ciencias, Universidad de Granada, Avenida de Fuentenueva, 18002-Granada, Spain*
[c] *Departamento de Química Orgánica, Facultad de Ciencias, Universidad de Granada, Avenida de Fuentenueva, 18002-Granada, Spain*

† Electronic supplementary information (ESI) available: Cartesian coordinates and intrinsic energies for all the calculated structures. See DOI: 10.1039/c0nj00171f

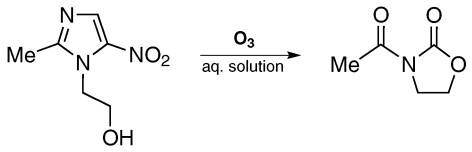

1
Metronidazole (MNZ)

2
N-acetyl-oxazolidin-2-one

Scheme 1 The ozone-mediated transformation of metronidazole (**1**) into *N*-acetyl-oxazolidin-2-one (**2**).

evaluation of the formation of stable *N*-acetyl-oxazolidin-2-one (**2**), see Scheme 1. Thus, compound **2** could be considered as an adequate contaminant indicator for nitroimidazoles in the ozonation processes of wastewaters, since **1** is the most frequently detected nitroimidazole therein. The mechanism involved in this conversion has also been postulated and calculated by means of DFT/B3LYP calculations in order to ascertain the most favorable pathway connecting both products.

Experimental

Reagents

All of the chemical reagents used were high-purity analytical grade reagents. Solutions were performed using ultrapure water.

Ozonation setup

The experimental system for nitroimidazole ozonation basically consisted of an ozone generator, a 2 litre reactor with agitator and UV-Vis spectrophotometer. Ozone was generated from oxygen by means of an ozonator with a maximum capacity of 76 mg min^{-1}. The reactor was covered for temperature control and was equipped with gas inlet and outlets, agitation system, and reagent and sampling dispensers.

In each experiment, the reactor was filled with 2 L of 50 mM phosphate-regulating solution at pH = 2. Once ozone partial pressure and temperature (25 °C) were adjusted, ozone was supplied to the reactor for 35 min until saturation of the solution. Then, 15 mL of concentrated metronidazole solution was injected to obtain the desired initial concentration in the reactor (10 mg L^{-1}). The ozonation reaction was stopped bubbling a stream of N_2 (g) for 5 min. In order to detect oxidation by-products generated in the metronidazole ozonation process, aqueous solutions obtained after different treatment times were extracted with Cl_2CH_2 and concentrated by using a rotary evaporator.

Analytical methods

Dissolved ozone concentration was colorimetrically determined by the karman-indigo method.[14]

Separation of ozonation by-products of antibiotics compounds from waters was performed using HPLC [equipped with a C18 analytical column (3.9 × 150 mm, 4 μm)]. Ammonium acetate 5 mM at pH 4.3 and acetonitrile were used as the mobile phases A and B, respectively. The mobile phase gradient elution was programmed as follows: 6% B during 10 min, from 6% to 30% in 10 min and kept during 3 min, and from 30% to 6% in 1 min. A 6 min re-equilibration time was used after each analysis. The flow rate used was set at 0.20 mL min^{-1} throughout the gradient. The column temperature was kept at 25 °C and the injection volume was 10 μL.

The HPLC system was coupled to a micrOTOF, an orthogonal-accelerated time-of-flight mass spectrometer (oaTOF-MS), equipped with an electrospray ionization (ESI) interface. Parameters for analysis were set using positive ion mode with spectra acquired over a mass range from m/z 50 to 1000. The optimum values of the ESI-MS parameters were: capillary voltage −4.5 kV; drying gas temperature 190 °C; drying gas flow 7.0 L min^{-1} and nebulizing gas pressure 21.7 psi.

The accurate mass data of the molecular ions were processed with the DataAnalysis 3.3 program, which provided a list of possible elemental formulas by using the Generate-MolecularFormula™ Editor. This program uses a CHNO algorithm, which provides standard functionalities such as minimum/maximum elemental range, electron configuration, and ring-plus double bonds equivalents, as well as a sophisticated comparison of the theoretical with the measured isotope pattern (Sigma-Value™) for increased confidence in the suggested molecular formula. It should be mentioned that even with very high mass accuracy (<1 ppm) many possible chemical formulae could be obtained depending on the mass regions considered. So, high mass accuracy (<1 ppm) alone is not enough to exclude enough candidates with complex elemental compositions. The use of isotopic abundance patterns as a single further constraint removes >95% of false candidates. This orthogonal filter can condense several thousand candidates down to only a small number of molecular formulas.

During the development of the HPLC method, external instrument calibration was performed using a syringe pump directly connected to the interface, passing a solution of sodium formate cluster containing 5 mM sodium hydroxide in the sheath liquid of 0.2% formic acid in water/isopropanol 1 : 1 (v/v). Using this method, an exact calibration curve based on numerous cluster masses each differing by 68 Da ($NaCHO_2$) was obtained. Due to the compensation of temperature drift in the micrOTOF, this external calibration provided accurate mass values (better than 5 ppm) for a complete run without the need for a dual sprayer setup for internal mass calibration.

Ionic chromatography was used for nitrite and nitrate anion determinations. Total organic carbon was used for the CO_2 determination.

Computational details

The calculations were carried out at the DFT-B3LYP level[15–17] with the Gaussian 03 program.[18] The geometries were fully optimized by the gradient technique using the standard 6-311+G(d,p) basis set,[19,20] which incorporates polarized functions for all the atoms and diffuse functions only for non-hydrogen atoms. The nature of the optimized structures, either transition states or intermediates, was assessed through a frequency calculation. We also report enthalpy and free energy values (not BSSE corrected), which

were obtained by taking into account the zero-point energies and the thermal motion at standard conditions (temperature of 298.15 K, pressure of 1 atm).

Results and discussion

The addition of **1** to an ozone-saturated, ultrapure aqueous solution led to the disappearance of the substrate after 10 min, although the reaction—taking into account the evolution of the possible by-products—remained completely stable after about 60 min. The residual ozone was removed by bubbling a stream of nitrogen for 5 min. and the resulting water solution was extracted with CH_2Cl_2. Gas chromatography revealed the apparition of a single product with a t_R = 6.5 min. Coupled low-resolution mass spectra (LRMS) gave a molecular peak for the new product formed of 129 amu, displaying a fragmentation pattern that fitted to oxazolidinone **2**. Furthermore, a rapid, direct-infusion electrospray mass spectrometry (ES-MS) technique was used to identify all the products formed in this reaction. Only the product **2** could be detected, obtaining a $[M + Na]^+$ peak of 152.0382 amu, thus indicating a $C_5H_7NO_3$ formula for the product. This structure was completely ascertained by means of the corresponding ^{1}H-NMR spectrum, realized from the mentioned organic extract.[21]

The ozone treatment has been always performed on ultrapure water solutions at pH = 2, adding *t*-BuOH (0.1 M) as radical scavenger. These conditions warrant a *direct reaction* of ozone, avoiding by this manner the radical pathway that may operate at different reaction conditions (neutral or basic pH, and absence of radical inhibitors). In fact, we were able to properly discriminate between the two mechanisms since the velocity constants are very different for each case. Thus, for the *direct reaction*, k_{O3} for **1** amounted to 82 ($\pm$1) M^{-1} s^{-1} at pH = 2, whereas this value rose to 4.4 ($\pm$0.2) 10^{10} M^{-1} s^{-1} at pH = 9.[21] Even under *direct reaction* conditions, ozone readily and irreversibly transformed the reactant (**1**) into the final detected product (**2**), and no other stable subproducts were detected by changing reaction times, always finding a perfect correlation between the disappearance of the reactant and the apparition of the product. This fits with a unique reaction pathway operating along the potential surface region in which is located the starting material. These findings moved us to consider the observed product as a convenient indicator for the presence of nitroimidazoles in ozone-treated wastewaters. Indeed, the ozonation of purchased oxazolidinone **2** indicated a very low rate constant for its degradation by ozone, k_{O3} being only 0.03 M^{-1} s^{-1}. This value is much lower than that obtained for **1**, meaning that, once the decomposition of **1** takes place, the concentration of compound **2** remains almost invariable during the ozonation process.

In order to evaluate the presence of other intermediates or side-reactions for the **1** → **2** transformation, we have checked the decomposition of MNZ (**1**) performing several HPLC-ESI-TOF(MS) experiments at different ozonation times. The detected products always were related products either with **1** or with **2**, also corroborating the unique process linking the two products. Thus, Fig. 1 shows the base peak chromatogram (BPC) at 0, 2, 3, 10, 20, 40 and 60 min during the MNZ degradation.

The present method is able to detect three compounds, namely (a) 2-methyl-1*H*-imidazole ($[M + H]^+_{exp.}$ 83.0598 *m*/*z*), (b) oxazolidin-2-one ($[M + H]^+_{exp.}$ 88.0391 *m*/*z*), and (c) MNZ (**1**) ($[M + H]^+_{exp.}$ 172.0717 *m*/*z*). Many data related with these compounds such as their migration time, formula, selected ion, experimental and calculated *m*/*z*, error (ppm and mDa), sigma value, tolerance, and the classification order considering other possibilities are summarized in Table 1 (see also Fig. 1).

TOF(MS) provides excellent mass accuracy over a wide dynamic range and allows measurements of the isotopic pattern, providing important additional information for the determination of the elemental composition. Therefore, all the detected compounds exhibit good sigma values (smaller than 0.05) and mass accuracy (ppm and mDa), see Table 1. Note that the products detected are directly related either with **1** or **2** and, therefore, no competing mechanisms seem to operate in this case.

We then decided to theoretically study the possible pathway connecting both products in order to establish not only the possible reactions involved therein but also the thermodynamics of such a process. For this purpose, a DFT/B3LYP computational study was performed using the standard 6-311+G(d,p) basis set, see the above Computational details section. Our guideline for the probable mechanism has been based on the postulated mechanism displayed in Scheme 2.

For this reaction, an enthalpy change of −214.6 kcal mol^{-1} has been calculated, indicating an irreversible and relatively high exothermic process. We have also calculated the free energy change since a significant gain for this magnitude is expected due to the change in the number of moles on each side of the general equation:

1 ($C_6H_9N_3O_3$) + O_3 + H_2O → **2** ($C_5H_7NO_3$) + HNO_2 + CO_2 + NH_3

H = –925.787223 kcal mol^{-1} H = –926.129197 kcal mol^{-1}

It has been experimentally observed the presence of two equivalents of nitrate ions (0.31 mmol from 0.15 mmol of **1**) coming from the two processes indicated in Scheme 2, namely the elimination of a nitrite ion after the ozonide formation (**4** in Scheme 2), and the hydrolysis of the final imine (**9** in Scheme 2) generating ammonia, both species being readily oxidized by ozone. Moreover, a total organic carbon (TOC) analysis revealed the presence of 1.28 mg L^{-1} of CO_2, just coming from the theoretical 1.52 mg L^{-1} of CO_2 that should be expelled in the **8** → **9** transformation. The postulated mechanism seems then to be coherent enough with the experimental findings.

DFT mechanism

The first step consists of a 1,3-dipolar cycloaddition of ozone to the nitroimidazole **1**. Although many positions may at first sight appear as accessible for ozone, only one allows a low-energy process: the C–C double bond. This is the preferred pathway to form the corresponding molozonide **3**. Furthermore, this process is highly stereoselective since the ozone

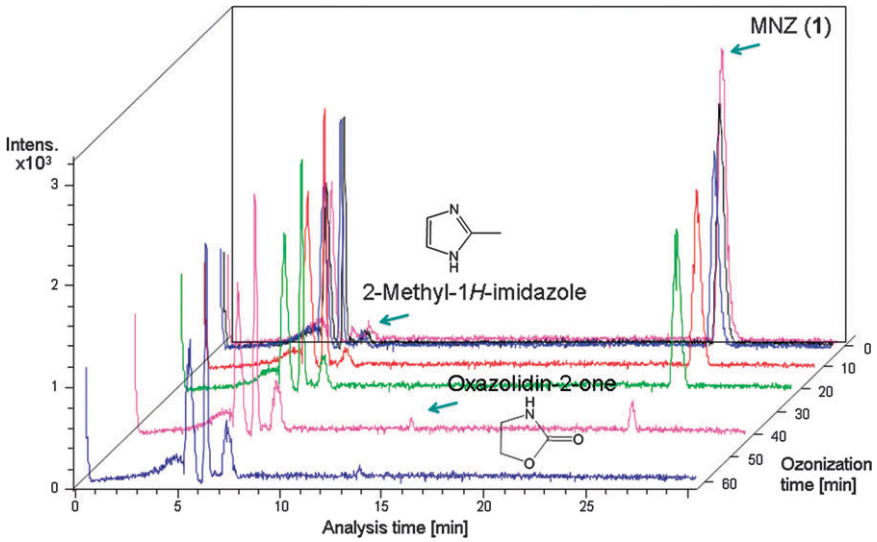

Fig. 1 Tridimensional HPLC-ESI-TOF(MS) diagram of the products found in function of the migration time and ozonation time.

Table 1 HPLC-ESI-TOF(MS) data for the detected compounds

Compound		2-Methyl-1*H*-imidazole	Oxazolidin-2-one	MNZ (**1**)
HPLC migration time/min		7.6	14.0	24.4
Formula		$C_4H_7N_2$	$C_3H_6N_1O_2$	$C_6H_{10}N_3O_3$
Selected ion		$[M + H]^+$	$[M + H]^+$	$[M + H]^+$
Exp. *m*/*z*		83.0598	88.0391	172.0717
Calc. *m*/*z*		83.0603	88.0393	172.0717
Error	ppm	6.7	2.0	0.1
	mDa	0.55	0.18	−0.01
Sigma value		0.0364	0.0260	0.0068
Tolerance (ppm) in GenerateMolecularFormula		10	5	5
Order on considering other possible compounds		1st of 1	1st of 1	1st of 3

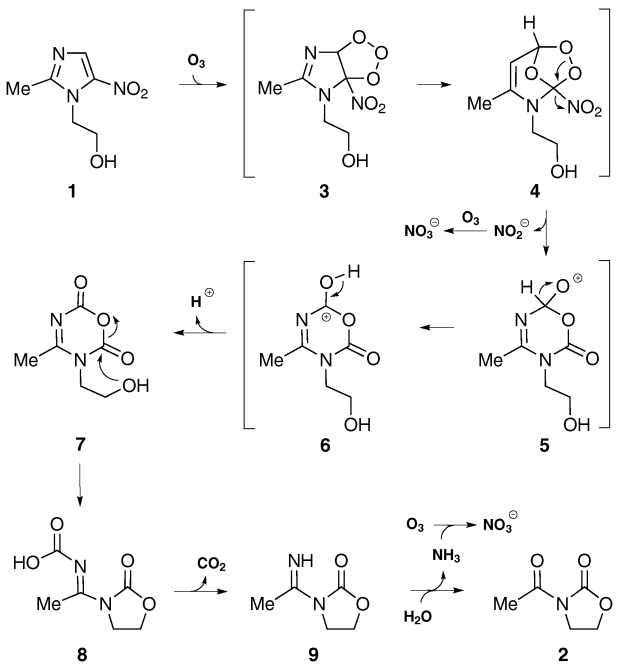

Scheme 2 The proposed mechanism for the conversion of **1** to **2**.

decidedly prefers, by 37.6 kcal mol^{-1} (enthalpy value), to be placed at the same side that the –CH_2CH_2OH chain, thanks to the hydrogen bond that can be established between them, see Fig. 2. The corresponding transition state enthalpy barrier for this process is quite low since the intrinsic ozone instability places the energy of the starting separated materials only 2.0 kcal mol^{-1} (enthalpy value) below, see Table 2. That the ozone preferably reacts with the C–C double bond can be drawn from the frontier molecular-orbital (FMO) theory.[22] Indeed, this fast, concerted 1,3-dipolar cycloaddition can be adequately viewed as the in-phase interaction between the C–C double bond HOMO (at −0.27039 hartree) and the ozone LUMO (at −0.20441 hartree),[23] through a $\pi \rightarrow \pi^*$ electron-donating process, see Fig. 3.

Several rearrangements have been essayed tempting to describe a low-energy molozonide re-organization to get the corresponding ozonide **4**, finding that the most favorable pathway corresponds in fact with that proposed by Criegee,[24] which in turn is the mechanism most widely accepted. This route begins with the molozonide rearrangement through the 1,2,3-trioxo unit breaking of the trioxolane ring. However, owing to the molecular asymmetry along the C–C double bond, we can consider two breaking ways: either (a) the

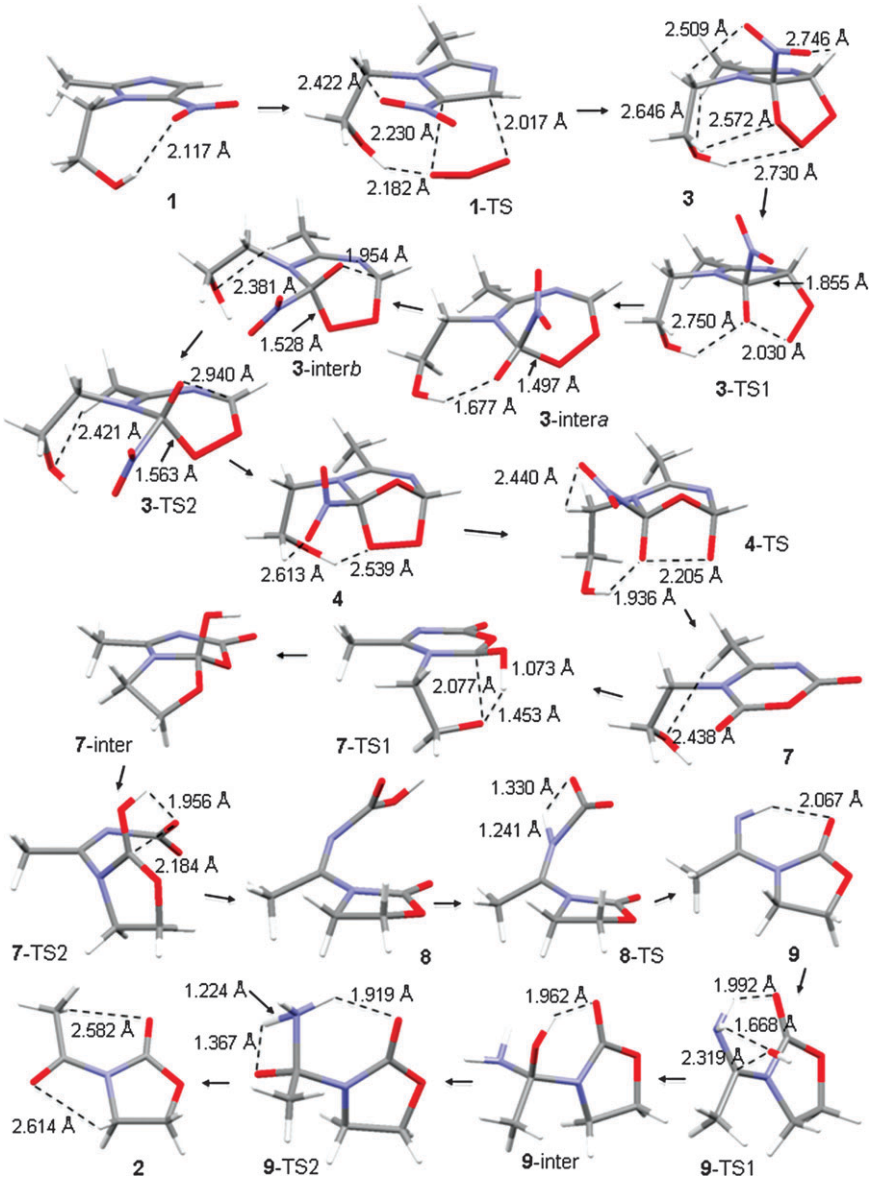

Fig. 2 A sequence of the calculated structures with some significant geometric parameters.

O–O fragment goes to the C–H carbon atom and the remaining O to the C–NO_2 carbon atom, or (b) the O–O fragment goes to the C–NO_2 carbon atom and the remaining O to the C–H carbon atom. The calculations showed that the most favorable pathway—by about 15 kcal mol^{-1}—corresponded to the (a) route, through the intermediates **3**-inter*a* and **3**-inter*b*, which are related by a simple CO(NO_2) rotation, see Fig. 2. This rotation has been calculated as slightly endothermic, see Table 2. The calculated energy values for the **3** to **4** transformation showed that, although the formation of the **3**-inter*a* intermediate is significantly exothermic, a very flat, reversible energy surface can be achieved on going from **3**-inter*a* to **4**.

But whereas the proposed mechanism (Scheme 2) displayed the intermediates **5** and **6**, calculations showed that the ozonide **4** could directly evolve—through the corresponding ozonide O–O fragment breaking process—to the carbamic anhydride **7** by the release of a molecule of HNO_2, the latter process running *with no activation barrier*.[25] The reason for this can be attributed to four interrelated factors: (a) the 1,3-diaxial disposition that the –NO_2 and –H groups acquire as the O atoms of the O–O fragment separate one from the other, (b) the more carbonyl character that these oxygen atoms gain with distance, (c) the subsequent leaving character that the –NO_2 group gets, and (d) the high exothermicity calculated for such a process (Table 2). This can be seen on the calculated $O_{carbonyl}$–C–NO_2 distance values on going from **4** to **7**, see Scheme 3. Note that during the process the –NO_2 group promotes a carbon to oxygen proton transfer in order to get an sp^2 C=O bond, all this progression occurring with no activation barrier.

Further intramolecular, nucleophilic attack of the oxygen atom of the –CH_2CH_2OH chain to the neighboring carbonyl group on **7**—through the somewhat high-energy four-membered transition state **7**-TS1 (see Fig. 2)—led to achieve the bicyclic intermediate **7**-inter. This process produces a

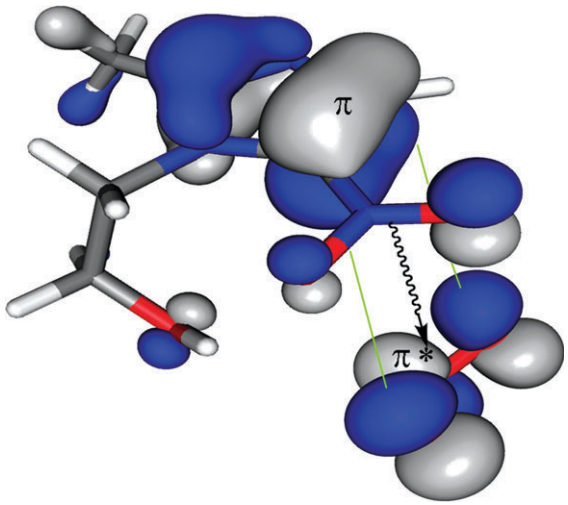

Fig. 3 Representation of the HOMO–LUMO π → π* electron-donating process between MNZ and ozone, respectively.

concomitant proton transfer to the mentioned carbonyl, see Fig. 2, generating a tertiary alcohol that lies 16 kcal mol^{-1} above the carbamic anhydride **7** (Table 2). This intermediate evolves, through a second four-membered transition state (**7**-TS2, which is about 7 kcal mol^{-1} lower in energy than the corresponding **7**-TS1 transition state, see Table 2), to the corresponding isomeric carbamic acid derivative **8**, see Fig. 2, which in turn is almost iso-energetic with the starting carbamic anhydride **7**.

From **8**, the subsequent CO_2 elimination process happens when a proton transfer takes place from the oxygen atom to the neighbor nitrogen atom, see Fig. 2. This then results in the moderately exothermic conversion of the original carbamic acid into the corresponding imine **9**, whose inevitable hydrolysis in the experimental conditions led to the final detected oxazolidinone **2**. This hydrolysis process operates following two steps: (a) the addition of a water molecule leading to the intermediate **9**-inter after a proton transfer reaction from the incoming water molecule to the present

Table 2 Calculated energies (Δ*E*), enthalpies (Δ*H*), and free energies (Δ*G*) for the species involved in the **1** → **2** transformation[a,b]

System	Δ*E*	Δ*H*	Δ*G*	Imaginary frequency[c]
1 + O_3	0.0	0.0	0.0	—
1-TS	+1.6	+2.0	+15.4	311[i]
3	−38.6	−36.9	−23.4	—
3-TS1	−34.7 (+3.9)[d]	−34.2 (+2.8)[d]	−20.4 (+3.0)[d]	246[i]
3-inter*a*	−77.4 (−38.8)[d]	−76.1 (−39.1)[d]	−63.1 (−39.6)[d]	—
3-inter*b*	−74.8 (−36.2)[d]	−73.2 (−36.3)[d]	−60.1 (−36.7)[d]	—
3-TS2	−65.2 (−26.6)[d]	−64.3 (−27.4)[d]	−50.1 (−26.7)[d]	351[i]
4	−77.1 (−38.5)[d]	−74.7 (−39.1)[d]	−60.5 (−39.6)[d]	—
4-TS	−51.3 (+25.8)[e]	−52.1 (+22.6)[e]	−38.7 (+21.8)[e]	301[i]
7[f]	−187.2	−186.6	−187.2	—
7-TS1	−137.2 (+50.0)[g]	−140.0 (+46.6)[g]	−138.5 (+48.8)[g]	985[i]
7-inter	−171.1 (+16.1)[g]	−170.6 (+16.0)[g]	−169.4 (+17.9)[g]	—
7-TS2	−146.2 (+41.1)[g]	−147.1 (+39.5)[g]	−146.7 (+40.5)[g]	241[i]
8	−186.6 (+0.6)[g]	−185.6 (+1.0)[g]	−185.8 (+1.4)[g]	—
8-TS	−150.0 (+41.1)[h]	−152.4 (+39.5)[h]	−153.0 (+40.5)[h]	1710[i]
9[i]	−200.0 (−13.4)[h]	−200.2 (−14.5)[h]	−211.1 (−25.3)[h]	—
9-TS1[j]	−165.2 (+34.8)[k]	−165.2 (+35.0)[k]	−165.0 (+46.2)[k]	435[i]
9-inter	−208.1 (−8.2)[k]	−205.6 (−5.4)[k]	−204.7 (+6.5)[k]	—
9-TS2	−171.5 (+28.5)[k]	−172.4 (+27.8)[k]	−172.3 (+38.9)[k]	1660[i]
2[l]	−214.6 (−14.6)[j]	−214.6 (−14.4)[j]	−226.7 (−15.6)[j]	—

[a] The values are in kcal mol^{-1}, the zero of energy (ZOE) for the whole reaction initially refers to the sum **1** + O_3. [b] The B3LYP total energy, enthalpy and free energy (in a.u.) are, respectively, for **1** + O_3: $E = -849.540145$, $H = -849.353822$, $G = -849.431477$. [c] In cm^{-1}, refers to the unique imaginary frequency of the calculated transition state. [d] Referred to **1** + O_3. The values in parenthesis refer to **3** as the ZOE for comparison. [e] Referred to **1** + O_3. The values in parenthesis refer to **4** as the ZOE for comparison. [f] Energy values referred to **1** + O_3 − HNO_2: $E = -643.768426$, $H = -643.606445$, $G = -643.655907$. [g] The values in parentheses refer to **7** as the ZOE for comparison. [h] The values in parentheses refer to **8** as the ZOE for comparison. [i] Energy values referred to **1** + O_3 − HNO_2–CO_2: $E = -455.121511$, $H = -454.974783$, $G = -454.999986$. [j] Energy values referred to **1** + O_3 − HNO_2 − CO_2 + H_2O: $E = -531.579974$, $H = -531.408184$, $G = -531.454809$. [k] The values in parentheses refer to **9** as the ZOE for comparison. [l] Energy values referred to **1** + O_3 − HNO_2 − CO_2 + H_2O − NH_3: $E = -474.997338$, $H = -474.863601$, $G = -474.887338$.

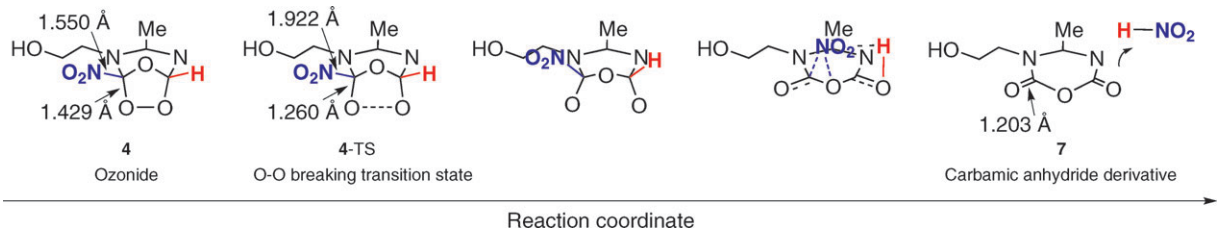

Scheme 3 The elimination of HNO_2 with no activation barrier from the corresponding O–O breaking transition state. The non-labeled structures have been obtained on relaxing the corresponding **4**-TS transition state.

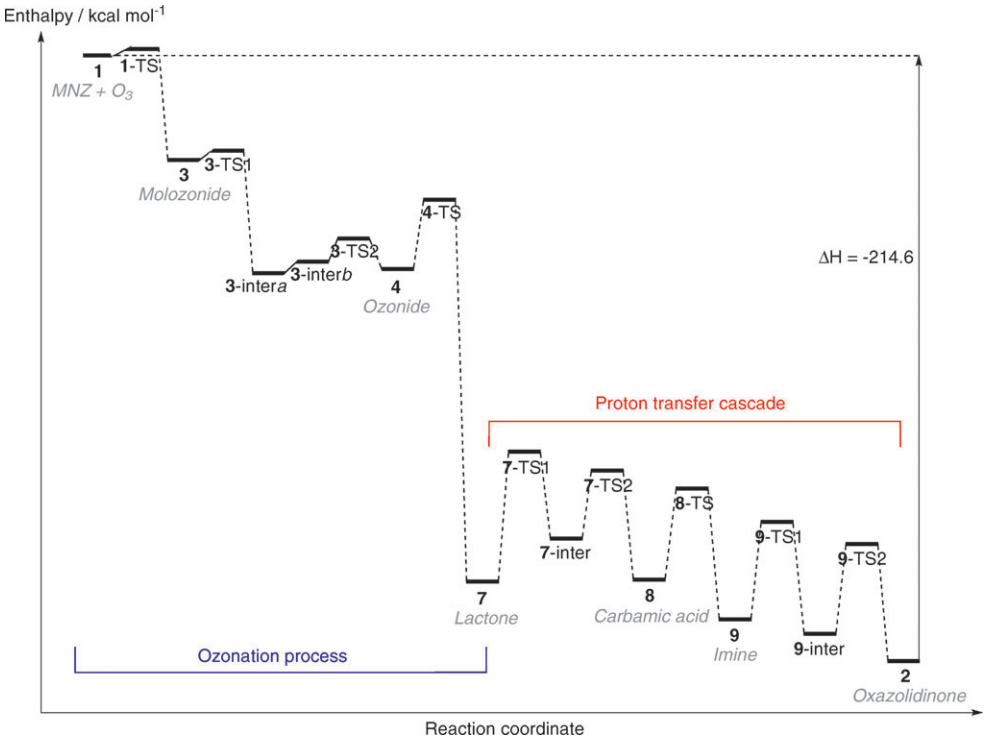

Scheme 4 The complete energy profile for the **1** → **2** transformation.

imine group, and (b) the elimination of ammonia thanks to a second proton transfer from the hydroxyl group to the amino group generated in the first step, see Fig. 2.

Note that the most part of the exothermicity of the studied reaction comes from the ozonation steps, since the energy of the carbamic anhydride **7**—formed just after the elimination of the HNO_2 molecule—is very close to the final energy calculated for the oxazolidinone **2**. It should also be noted that changes in the free energy values correspond, as expected, with the uptake and elimination of the small molecules that participate in the mechanism. The other processes are all intramolecular and, consequently, it takes place a small change in the free energy.

A complete view of the energy profile for the whole reaction can be seen in Scheme 4. Note the high exothermicity of the HNO_2 elimination (**4** → **7** conversion), and the proton transfer cascade pathway connecting structures **7** and **2**.

Conclusions

The use of *N*-acetyl-oxazolidin-2-one as a covenient indicator in the removal of nitroimidazoles—acting as antibiotic contaminants in wastewaters—has been studied since it is the sole degradation product achieved in the treatment of metronidazole-containing waters carried out by ozone, and it is stable against further ozonation in the experimental conditions used. This conversion has been extensively studied by different techniques in order to trap possible by-products and/or other subproducts. The ozone treatment, however, does not allow isolation of any by-products, the reactant being readily and irreversibly transformed into the final detected product. Nor were other stable subproducts detected, indicating that both the starting metronidazole and the final *N*-acetyl-oxazolidin-2-one are probably connected by a unique reaction pathway. Indeed, coupled HPLC-ESI-TOF(MS) revealed the presence of simple derivatives of both metronidazole and *N*-acetyl-oxazolidin-2-one, leading us to think that both substances are strongly interconnected and that no other stable species are implied in the conversion. A possible mechanism for this transformation has been then postulated and evaluated by DFT/B3LYP calculations, showing that the observed product should be readily obtained mainly thanks to the high exothermicity displayed by the ozone action over the metronidazole to obtain a lactone derivative that suffers a series of hydrolysis processes leading to the final product.

Acknowledgements

We thank MEC-DGI-FEDER (project CTQ2007-67792-C02-01/PPQ) and the Junta de Andalucía (projects RNM3823 and FQM03705) for financial support. D. Arráez acknowledges funds from the Consejería de Innovación, Ciencia y Empresa, Junta de Andalucía (project P07-AGR-02619). The calculations have been carried out at the Centro de Supercomputación de la Universidad de Granada (CSIRC, Granada, Spain). The authors wish to thank Javier Camino Sánchez from LVM Cavendish and Alegría Carrasco Pancorbo from University of Granada for their assistance in the analytical determinations carried out in this work.

References

1 M. L. Richardson and J. M. Bowron, *J. Pharm. Pharmacol.*, 1985, **37**, 1.
2 B. Halling-Sørensen, S. Nors Nielsen, P. F. Lanzky, F. Ingerslev, H. C. Holten, S. Lützhøft and S. E. Jørgensen, *Chemosphere*, 1998, **36**, 357.
3 D. Calamari, *Toxicology*, 2002, **181–182**, 183.

4 C. G. Daughton, *Environ. Impact Assess. Rev.*, 2004, **24**, 711.
5 K. Kümmener, *Chemosphere*, 2001, **45**, 957.
6 K. Kümmener, *J. Antimicrob. Chemother.*, 2004, **54**, 311.
7 K. Kümmener, A. Al-Ahmad and V. Mersch-Sundermann, *Chemosphere*, 2000, **40**, 701.
8 A. Bendesky, C. Menéndez and P. Ostrosky-Wegman, *Mutat. Res., Rev. Mutat. Res.*, 2002, **511**, 133.
9 R. Lindberg, P. Jarnheimer, B. Olsen, M. Johansson and M. Tysklind, *Chemosphere*, 2004, **57**, 1479.
10 F. P. Tally and C. E. Sullivan, *Pharmacotherapy*, 1981, **1**, 28.
11 A. H. Lau, N. P. Lam, S. C. Piscitelli, L. Wilkes and L. H. Danziger, *Clin. Pharmacokinet.*, 1992, **23**, 328.
12 A. Wennmalm and B. Gunnarsson, *Drug Info. J.*, 2005, **39**, 3.
13 M. Carballa, F. Omil, J. M. Lema, M. Llompart, C. García-Jares, I. Rodríguez, M. Gómez and T. Ternes, *Water Res.*, 2004, **38**, 2918.
14 H. Bader and J. Hoigné, *Water Res.*, 1981, **15**, 449.
15 A. D. Becke, *Phys. Rev. A: At., Mol., Opt. Phys.*, 1988, **38**, 3098.
16 C. Lee, W. Yang and R. G. Parr, *Phys. Rev. B: Condens. Matter*, 1988, **37**, 785.
17 A. D. Becke, *J. Chem. Phys.*, 1993, **98**, 5648.
18 M. J. Frisch, G. W. Trucks, H. B. Schlegel, G. E. Scuseria, M. A. Robb, J. R. Cheeseman, J. A. Montgomery, Jr., T. Vreven, K. N. Kudin, J. C. Burant, J. M. Millam, S. S. Iyengar, J. Tomasi, V. Barone, B. Mennucci, M. Cossi, G. Scalmani, N. Rega, G. A. Petersson, H. Nakatsuji, M. Hada, M. Ehara, K. Toyota, R. Fukuda, J. Hasegawa, M. Ishida, T. Nakajima, Y. Honda, O. Kitao, H. Nakai, M. Klene, X. Li, J. E. Knox, H. P. Hratchian, J. B. Cross, V. Bakken, C. Adamo, J. Jaramillo, R. Gomperts, R. E. Stratmann, O. Yazyev, A. J. Austin, R. Cammi, C. Pomelli, J. Ochterski, P. Y. Ayala, K. Morokuma, G. A. Voth, P. Salvador, J. J. Dannenberg, V. G. Zakrzewski, S. Dapprich, A. D. Daniels, M. C. Strain, O. Farkas, D. K. Malick, A. D. Rabuck, K. Raghavachari, J. B. Foresman, J. V. Ortiz, Q. Cui, A. G. Baboul, S. Clifford, J. Cioslowski, B. B. Stefanov, G. Liu, A. Liashenko, P. Piskorz, I. Komaromi, R. L. Martin, D. J. Fox, T. Keith, M. A. Al-Laham, C. Y. Peng, A. Nanayakkara, M. Challacombe, P. M. W. Gill, B. G. Johnson, W. Chen, M. W. Wong, C. Gonzalez and J. A. Pople, *GAUSSIAN 03 (Revision B.04)*, Gaussian, Inc., Wallingford, CT, 2004.
19 R. Krishnan, J. S. Binkley, R. Seeger and J. A. Pople, *J. Chem. Phys.*, 1980, **72**, 650.
20 A. D. McLean and G. S. Chandler, *J. Chem. Phys.*, 1980, **72**, 5639.
21 M. Sánchez-Polo, J. Rivera-Utrilla, G. Prados-Joya, M. A. Ferro-García and I. Bautista-Toledo, *Water Res.*, 2008, **42**, 4163.
22 K. Fukui, in *Theory of orientation and stereoselection*, Springer-Verlag, Heidelberg, 1970 (revised edn 1975). See also: (*a*) K. Fukui, *Pure Appl. Chem.*, 1982, **54**, 1825; (*b*) K. Fukui, *Science*, 1987, **218**, 747.
23 A. H. Pakiari and F. Nazari, *THEOCHEM*, 2003, **640**, 109.
24 R. Criegee, *Angew. Chem., Int. Ed. Engl.*, 1975, **14**, 745.
25 We have arrived to this conclusion from several calculations on the corresponding **4**-TS transition state observing that a low-energy pathway, directly leading to the lactone **7**, can be obtained accompanied by the release of the HNO_2 species. Note that during the process the $-NO_2$ group promotes a carbon to oxygen proton transfer in order to get an sp^2 C═O bond.

